SSC20-WKVIII-01

Antennas for Academic CubeSats: VHF thru S-Band, What, How and Why

Albert E. Lyerly, Peter W. Pachowicz
George Mason University
Department of Electrical and Computer Engineering, MS 1G5
4400 University Dr., Fairfax, VA 22030; 703-404-7439
alyerly@masonlive.gmu.edu ppach@gmu.edu

ABSTRACT

This work is dedicated to teams which want to build and fly their own antennas. Frequencies covered include VHF, UHF, L-band and S-band, while antenna types include monopole, dipole, J-pole, 5x5cm patch, and fractal patch. Antennas were simulated, built, attached to a satellite mockup, and tested in an anechoic chamber at the Northrop Grumman facilities. Simulation results and obtained test results are presented to support the teams in designing their own antennas and to provide guidance and verification of realistic performance expectations.

1. INTRODUCTION

This paper is dedicated to teams facing dilemmas when designing and building antennas for their own CubeSats. While there is a large collection of fundamental and simulation data that help the antenna designer, other factors such as the implementation, CubeSat body and space environment, have significant influence on realistic antenna performance. Teams that followed only simulation results were frequently disappointed by an in-flight underperformance of their communication systems. In understanding the reasons behind such an underperformance, teams need to focus first on a front-end of their communication system; i.e., satellite antennas. Driving motivation behind this extensive work was based on practical aspects of antenna construction rather than mathematical foundations which can be found in many textbooks [1, 2]. We also limit this work to simple antenna structures rather than on new trends for CubeSat antennas [3].

In assisting academic teams, we provide a compilation of lessons learned and recommendations based on simulations and results obtained from designing and testing various antenna prototypes. Frequencies covered in this paper include VHF, UHF, L-band and S-band, while antenna types include monopole, dipole, J-pole, 5x5cm patch, and fractal patch. Antennas were built, attached to a satellite mockup, and tested in an anechoic chamber at the Northrop Grumman facilities. Since for most teams, gaining an access to a full scale antenna testing facility is mostly impossible, these results could provide a guidance and verification (actually understanding a degree of derating) of their expectations. The results presented combine simulation and testing curves while we comment on influencing factors. We stress realistic expectations and parameter change/deterioration regarding gain and bandwidth due to the presence of the satellite body, space induced temperature variations, and the importance of space qualified material choices. This extensive study should help teams in avoiding mistakes and defining practical values for antenna gain, bandwidth and overall antenna performance parameters. We also discuss secondary effects such as transmit antenna generated electromagnetic interference due to antenna choice, antenna pattern, and antenna placement within the CubeSat structure. Recommendations provided are based on many years of work with different antennas at Northrop Grumman (former Orbital Sciences).

2. VHF/UHF WIRE ANTENNAS

The VHF/UHF bands are typical frequencies for commanding uplinks and telemetry downlinks. In our study, however, we focus on the amateur radio UHF sub-band and simple wire-based antennas. We only provide some recommendations regarding the VHF sub-band without designing and testing specific VHF antennas.

2.1 VHF Sub-Band

The VHF frequencies, especially for amateur satellites, were very frequently used in the past. For AMSAT satellites utilizing SSB, CW and digital modes VHF is still the frequency of choice. There are several reasons behind the utilization of VHF, such as: a full-duplex

voice communication using the B-mode (UHF/VHF) and wide spread availability of typical radio equipment.

However, a new trend already in place is to move into higher frequencies where more bandwidth is available (VHF satellite bandwidth of 200 kHz vs. UHF satellite bandwidth of 3 MHz). Also, the VHF band became really crowded and thus there is increased receiver interference. But the main reason behind the transition to UHF is ever increasing noise level on VHF. Ground household equipment, such as uncertified LED light bulbs and plasma TVs, create problems for ground receivers in urban areas. Also long-range high-power military radars create problems for satellite receiver (also for the UHF receivers [4]). Another reason is the availability of ultra-low power transceiver chips for UHF frequencies. Therefore, our recommendation is to skip the VHF and focus on the UHF for satellite commanding and telemetry communications.

2.2 UHF Monopole Antenna

The construction of monopole wire antenna is very simple. It includes selecting and cutting a wire to the λ/4 length and providing a perpendicular ground plane of λ/2 diameter. For a 17.5 cm monopole, the requirement for the ground plane formed by parallel satellite surface is 35 cm, what cannot be achieved for small CubeSat. This will require experimental tuning through gradual cutting the length of the wire into desired return loss measurement. Good results can be achieved because the monopole antenna can be quite forgiving in reaching desired return loss. However, the radiation pattern of such a setup may not be omni-directional. Proper testing in an anechoic chamber should follow to verify antenna radiation pattern to avoid in-flight surprises.

The ground plane is created by satellite external panels and have to be constructed to provide electrical connectivity. Since RF current will flow through these panels, one naturally expects a higher level of Electro-Magnetic Interference (EMI) influencing operations of internal and external electronics. This influence is most significant during transmission and makes sensors reading and bus voltages (especially I2C bus) unreliable. This can also influence transmitter electronics and microcontroller controlling the transmitter, if proper electromagnetic shielding is not in place

2.3 UHF Dipole Antenna

The advantages of dipole antenna for UHF band and placed on small CubeSats are multifold:

- Almost omni-directional characteristics with approximately 360° coverage in the normal plane to the dipole axial axis
- Inherited reduced ground station antenna pointing accuracy is not needed
- Easily constructed using two spring wires (or tapes) forming total antenna length of λ/2
- Linear and circular polarizations can be implemented
- Simple trimming antenna arm lengths used to tune the antenna to specific frequency
- Impedance bandwidth can range from 2% to 15% without any decrease in gain
- Many different methods for stowage and antenna deployment have already been tested in space environment

Arms of the dipole antenna should be constructed from Nitinol spring wire. However, Nitinol wire is a steel-type wire which has an electrical resistance higher than copper and thus the antenna engineer must compensate antenna design for this loss.

For modeling using ANSYS HFSS simulator a Nitinol wire of 0.394 mm and electrical conductivity of 1.10 x 10^6 Siemens/m was used. Due to our interest in 0.5U CubeSat, modeling included a 10x10x5 cm CubeSat structure made of smooth and seamless conductive copper with conductivity of 5.96 x 10^7 Siemens/m. The dipole antenna was mounted on 1.58 mm FR4 material. The desirable location for the mounted dipole is the corner of the 0.5U CubeSat structure as shown in Figure 2.1. This is a desirable location to mount the dipole because it allows a workable stowage of the dipoles by coiling each dipole arm on the top of the CubeSat. This is why Nitinol wire has been a popular choice for dipole arms. Dipole arms are also clear of the CubeSat body to maintain good linear polarization. The dipole is fed with a voltage source of internal impedance of 50 ohms.

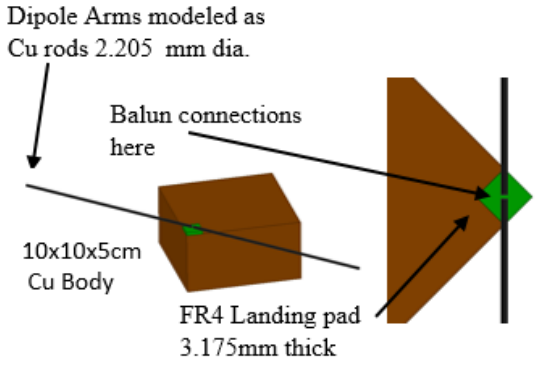

Figure 2.1: Model of the UHF Dipole Antenna

The length of the antenna should resonate at approximately *0.9*c/2*, where *c* is the free space wavelength of the dipole. For this design, the antenna length was set to be *c/2* and trimmed gradually to achieve the resonance. Resonance of the dipole implies the dipole impedance radiation resistance will be real with no capacitive or inductive components in the impedance. However, this is not the case, the dipole impedance will be real only at a single frequency of 436.5 MHz. To minimize the reactive swing, the antenna will be tuned to the center of the band, thus we try to "balance" the imaginary part of the impedance. Figure 2.2 shows dipole impedance from 400.0 MHz to 470.0 MHz as plotted on the Smith Chart. The Smith Chart shown is normalized to $Z_{normalized}$ = 73.0 + j0 ohm, thus we see at the design frequency of 436.5 MHz the $Z_{normalized}$ = 1.0 + j0 ohm. The predicted dipole length for 436.5 MHz was 34.25cm. The adjusted free-space resonance was 32.21 cm. This is representing an error of 6.3%.

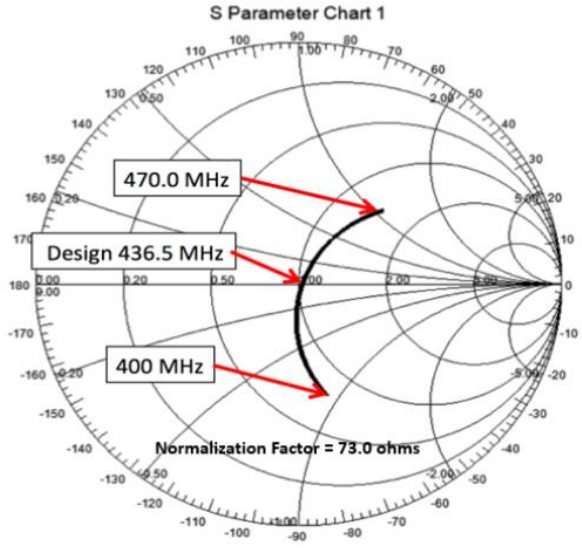

Figure 2.2: UHF Dipole in Free Space vs Frequency

The modeling of the dipole to determine the input impedance was expanded to compare the dipole in the follow three conditions: (1) Dipole impedance in free space at fixed length 32.13 cm, (2) Dipole impedance corner mounted on the 0.5U CubeSat of fixed length 32.13 cm, and (3) Dipole retuned to resonance corner mounted on the 0.5U CubeSat of fixed length 33.71 cm. Figure 2.3 shows a frequency shift of the free-space designed dipole from 436.5 MHz to the 0.5U CubeSat mount to 448.0 MHz. The frequency shift is due to the capacitive coupling of the dipole to the structure. This is by inference, since the dipole changed from free-space operation to operating in the presence of the conductive CubeSat body. This frequency shift puts the dipole outside of its design range. Modeled electrical performance shows the dipole will be longer from the baseline length by 4.9% as summarized in Table 2.1. This implies the resonant equation formula is not adequate when a dipole is placed on the structure. Thus, for proper CubeSat dipole operation, the modeling must include CubeSat structure and dipole must be tested and proper adjustments must be made.

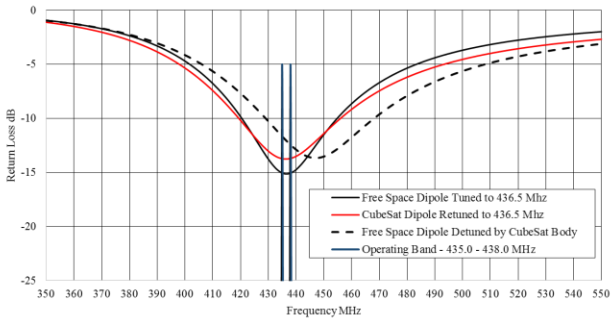

Figure 2.3: Model Dipole Resonance Comparison

Table 2.1: Free Space Dipole Length vs 0.5U CubeSat Dipole Length

Nitinol Dipole Arm Description	Environmental Conditions	Length [mm]	Resonant Frequency [MHz]	Dipole Length Correction [%]
Baseline Tuned to Free Space	Free Space	321.32	436.5	0.0
Tuned to Free Space	0.5U CubeSat Corner Mount	321.32	438.0	0.0
Tuned to 0.5U CubeSat Structure	0.5U CubeSat Corner Mount	337.14	436.5	-4.9

The CubeSat will experience a temperature shift in space during its mission of -35C to +85C. To maintain the dipole in resonance, it is importance to build the dipole with either: a) Low coefficient of expansion material, or b) Wide bandwidth match to compensate for the temperature swing.

In dipole operation and design, the increase in dipole arm thickness will increase the dipole impedance bandwidth. Figure 2.4 demonstrates the widening of the

dipole impedance match for 0.5U CubeSat in the corner-placed dipole model of three various dipole wire diameters. The dipole wire diameter steps from 0.401 mm diameter Nitinol wire up a ¼ inch tape. The Modeling shows -10 dB Bandwidth increased from 9.4% to 17.2 %. Since the 0.401 mm Nitinol Wire meets the UHF Bandwidth requirement of 435.0 to 438.0 MHz bandwidth, the Nitinol wire can be used as the dipole arm material for the 0.5U CubeSat.

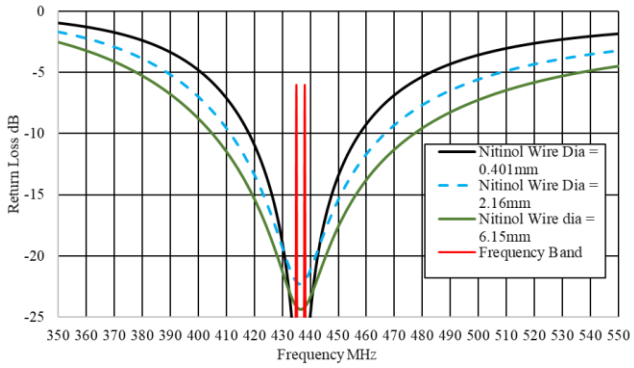

Figure 2.4: Dipole Impedance of Dipole Bandwidth vs Dipole Arm Thickness

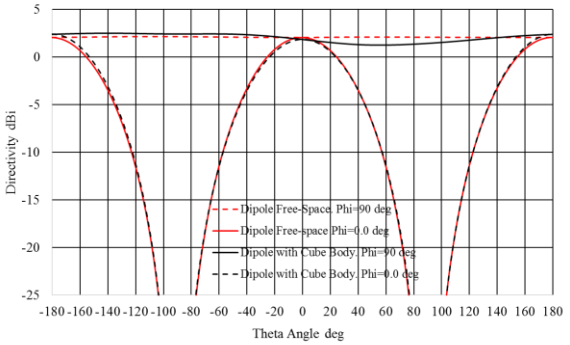

Figure 2.5: Model Free Space Dipole vs 0.5U Corner Placed Dipole Plane Cuts

Further analysis is conducted to determine the significance of antenna blockage by the CubeSat body. The antenna blockage should be low since the UHF frequency wavelength is much larger than 0.5U CubeSat body. Figure 2.5 shows two plane electric field or E-field cuts at Phi = 0.0° (the dipole broadside axis) and Phi = 90.0° (the dipole axial axis.) There are four pattern cuts. The red dotted color cut is the baseline dipole radiating in free space. The proper dipole pattern behavior at Phi = 0.0° is a constant 2.2 dBi, what is actually shown. Adding the 0.5UCubeSat body, the spacecraft will block the wave causing a decrease in dipole directivity. This is clearly shown in the black solid line. The broken cuts show an antenna Directivity drop of approximately only 1.0 dB.

2.4 Performance of Constructed UHF Dipole Antenna

For simplicity of model building and maintaining electrical connections a 2.159 mm copper tube was used for experimentation (Nitinol is difficult to solder). The dipole was soldered to the corner side of a 0.5U CubeSat copper covered brass board model. The dipole antenna is placed in the corner to be as close to "flight like" position as shown on Figure 2.6. The dipole is fed with 0.141 semi-rigid 50 ohm coax cable. The 0.5U CubeSat body was made from cut double sided 1/8 inch thick copper clad circuit board. The cube is joined together with 1 inch copper tape. DC resistance was measured between each of the 6 copper walls with a mean value of <0.3 ohm. The coax cable connector is an SMA female type. A 1:1 Balun (PN: CX2078NL) is fed at the dipole feed point (Figure 2.7). The Balun is solder to 1/8 inch copper board with connection traces cut with an Exacto knife to accommodate the solder-in Balun. The dipole was tuned with the Agilent E8353ES network analyzer.

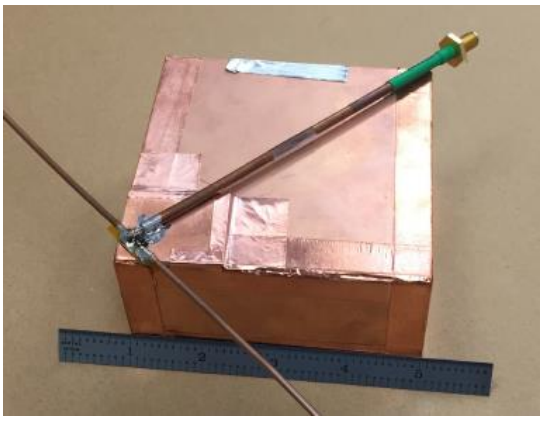

Figure 2.6: UHF Antenna Positioned on the 0.5U structure

Measuring return loss and tuning of the Dipole was conducted in the Northrop Grumman, Dulles Campus Anechoic Antenna Range. The room contained 9 inch Emerson and Cummings pyramidal absorber (VHP-8-NRL) that is rated at 30 dB at 1 GHz. Between the 350 to 550 MHz band, the published absorber loss is approximately 10-20 dB. The initial dipole resonance was a bit higher than 436.5 MHz and small trimming of both ends of the dipole was required. The result is shown in Figure 2.8. Measured vs modeled performance shows close agreement.

Figure 2.7: Close up of Balun Connection

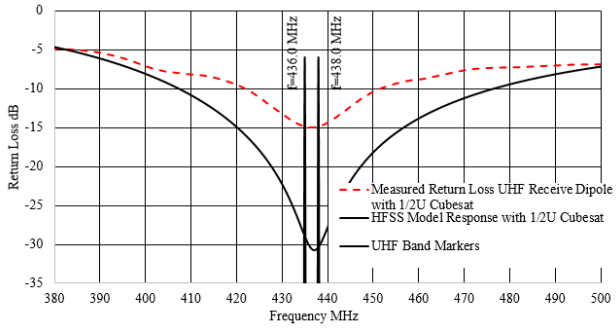

Figure 2.8: Measured vs Model UHF Dipole Return Loss in 0.5U CubeSat Configuration

3. L-BAND J-POLE UPLINK ANTENNA

The AMSAT 144 and 430 MHz CubeSat frequency bands are very popular communication bands shared by the amateur terrestrial and amateur satellite users, however, these frequencies are prone to increased unintentional jamming from these terrestrial sources and nearby CubeSat operators. The AMSAT L-band frequency of 1260-1270 MHz is less crowded than the lower AMSAT frequencies and provides an attractive alternative for an uplink frequency band to be considered. (Please notice that a downlink operation is not permitted by the ITU and AMSAT on the L-band.)

3.2 The J-Pole Antenna

The linearly polarized J-pole antenna is an interesting alternative to the monopole for operating in the L-band frequencies. The benefits of the J-Pole when placed on small CubeSat are: (1) Antenna length to project the antenna away CubeSat body and thus benefit from minimal signal blockage by the CubeSat body, (2) Almost omni-directional radiation pattern, and (3) No need for an antenna ground plane which will be the CubeSat body. The antenna length is about *3/4*λ*, corresponding to ~17 cm. The geometry of the antenna and careful antenna deployment placement on the Cubesat body will assure minimal receive signal blockage from the ground station to the Cubesat antenna.

The J-pole is a linear polarized antenna consisting of a half wavelength dipole fed at the end tip by a short circuit parallel wire ¼ λ transmission line (see Figure 3.1). As seen, a clear benefit of the J-pole is the absence of an electrical attachment to the CubeSat body performing as the antenna ground plane. The lack of an antenna ground plane is due to the antenna RF currents directed thru the short circuit of the ¼ λ matching stub assembly and not the CubeSat (such as for a monopole antenna.)

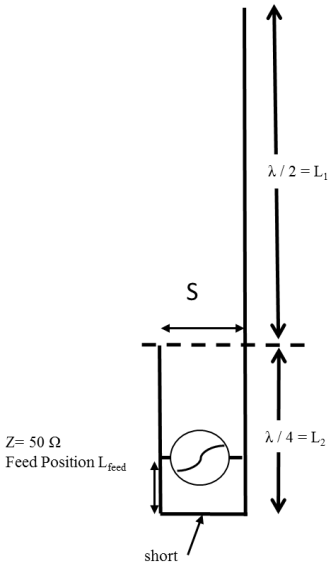

Figure 3.1: End Fed Dipole Known as the "Zepp" Antenna [2][5]

For the J-pole, we would like to excite the antenna at the λ/2 dipole tip end. The dipole end is a current minimum and a voltage maximum, thus the impedance approaches theoretically infinite resistance, from Ohms Law, $Z = V_{ant}/I_{ant}$ at the antenna tip (the impedance is >1000 ohms.) A practical method to feed the dipole end is to match the end with a quarter wavelength short circuit stub transformer. The short circuit stub transformer is a transmission line a quarter wavelength long with one end shorted and a quarter wavelength distance opposite is an open circuit. On the open circuit side of the short circuit transformer, the impedance is high (of >1000 ohms) and thus it conveniently matches to the half wavelength dipole tip. To match the receiver side of the antenna (the shorted end of the short circuit

stub is 0 ohm) one can intuitively see that moving away from the stub the line impedance will increase. We normally would like to feed the J-pole with Z_{gen} =50.0 + j0.0 ohm. Using the quarter wavelength short circuit stub as a transformer, we are able to achieve the 50.0 ohm impedance at L_{feed} by positioning the balanced feed point a fraction of a wavelength short from the short as shown in Figure 3.2. This distance can be approximated by the transmission line formula, by experiment or antenna modeling. The short circuit stub requires a balanced feed, thus in Figure 3.2 a Balun circuit is shown.

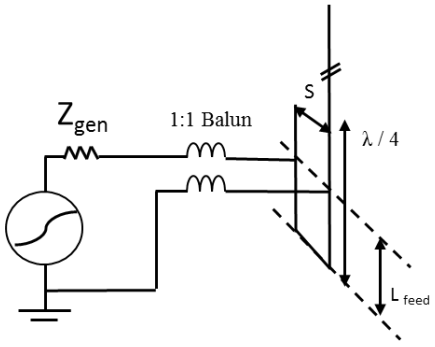

Figure 3.2: Feed Location for the J-Pole Antenna

3.2 J-Pole Antenna Development

A J-pole antenna featuring deployable friendly Nitinol wire is preferred for flight operation due to its memory spring properties. However, for this presentation, silver plated copper wire was built and the electrical performance presented. The use of the 20AWG wire for the J-pole elements presents practical stowage and deployment opportunities to the CubeSat user, however thinner gage wire may be used. To minimize the antenna detuning effects from temperature swings from the space environment, the desirable impedance bandwidth should be designed to be larger than the operating frequency. The key parameters of the development of the J-Pole antenna are summarized as follows:

(1) Establish the operating frequency, bandwidth operation and bandwidth over space temperatures.
(2) Estimate expected space environment temperature, radiation and UV exposure.
(3) Select wire gage and notional stowage and deployment approaches for this wire gage and type.
(4) Establish wire spacing with pre-knowledge that λ/4 transformer bandwidth to compensate for space temperature swings.
(5) Assume low RF loss support structure of the parallel wire quarter wavelength transmission line.

After the selection of the J-pole wire, the second step is to compute the free space half wavelength and quarter wavelength arms at the center of the operating band of the J-pole. The modern approach to the J-pole design is to use an electromagnetic modeling simulator. We used ANSYS HFSS ver19 to model and predict the antenna radiation pattern and antenna input return loss. Other electromagnetic modeling tools can be used such as the Numerical Electric Code (NEC), MiniNec and Ticra GRASP to name a few.

The last step in the design of the J-pole is to determine the support structure of the parallel transmission line. What is critical of the support structure is: (1) High reliable stowage and deployment of the antenna, (2) Low RF loss at the frequency of operation, and (3) Survivable to UV and the space environment. In this J-pole design, 0.1 mm Kapton tape was used to support and maintain parallel wire separation of the quarter wavelength short circuit stub transformer. Kapton was selected for its UV and space environment use and survivability. However, the stub length must be compensated and made shorter than the free space length due to the dielectric properties of the tape. Hence, modeling the support structure electrical and mechanical properties must be included in the design. For a low loss receive antenna, consideration of the loss properties is critical in the design and implementation of this antenna.

For reliable operation of the antenna over temperature, the antenna impedance bandwidth should be greater than the operating bandwidth of the antenna in order to compensate for impedance matching shift over temperature. The enlarged compensation bandwidth can be determined by analysis and confirmed by a temperature cycle test. The quarter wavelength stub spacing "S" (Figure 3.1) for proper impedance bandwidth of the J-pole was found through experimentation with ANSYS HFSS. The larger the spacing the increased impedance bandwidth. Figure 3.3 shows the trend for larger bandwidth in air. The three wiring spacing of 2.0, 1.28 and 0.63 mm are shown. The larger the wiring spacing, the increase in the –10 dB return loss bandwidth. As seen, the wiring spacing of 2.03 mm produces a bandwidth of 20 Mhz, double the required bandwidth.

The feed for the J-pole was selected to be a balanced generator of 50 ohm impedance. The feed location was determined numerically by using the parameter function of HFSS. The feed was moved beginning at the short of the short circuit stub and climbing away from the short

until 50 ohms was located. We observed the half wavelength J-pole length *L1* should be cut to the free space length of short circuit stub. The final feed position for 50 ohm impedance was found to be 3.10 mm from the short. The final J-pole design included Kapton tape, 0.127 mm thick that was used to dimensionally support the parallel wire short circuit stub. The antenna was tuned to the center frequency of 1.265 GHz. In the design, the parallel wire transmission line is supported with 2 layers of Kapton tape for a total thickness of 0.254 mm. The stowage and deployment method details are not included in this paper, however the Kapton tape and a Nitinol wire J-pole antenna has been successfully wrapped around the body of a Cubesat-like structure and deployed by the cutting of a silk containment tie.

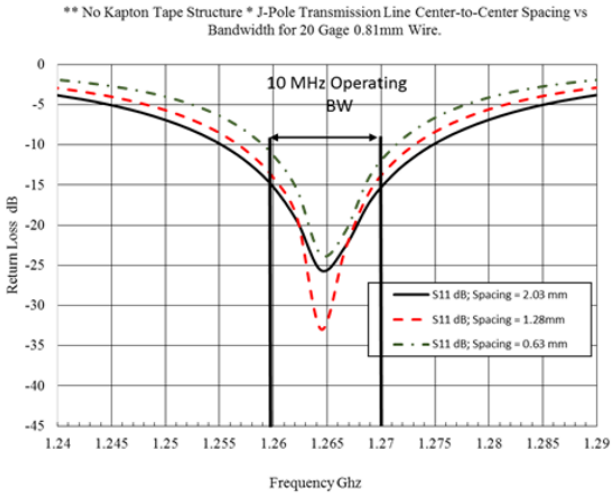

Figure 3.3: Wire Spacing vs Impedance Bandwidth in Air

Table 3.1: J-Pole Dimensions, Model vs As-Built

Parameter (mm)	Model (mm)	As-Built (mm)
Wire Diameter	0.813	0.813
L_{feed}	3.10	3.175
$S_{inner\ spacing}$	2.03	2.0
L_1	106.43	112.9
L_2	45.90	54.2
Kapton thickness	0.254	0.254

The J-pole model was built using the predicted dimensions given in HFSS as a starting point. Some adjustments were conducted to "tune" the antenna for a minimum Return Loss at the center frequency of 1265.0 MHz. We found the quarter wave length stub length to provide the most tuning range and tuning sensitivity. The half wavelength antenna length should be kept at its constant model predicted length. Very little to no frequency shift occurred when trimming the half wavelength antenna portion of the J-pole. Model dimensions are shown in Table 3.1 and the antenna is shown in Figure 3.4. The J-pole is fed by 0.141inch semi-rigid cable to a 1:1 MACOM Ferrite Bead Balun (PN: MABACT0059). The published insertion loss at 1265.0 Mhz is approximately 0.63 dB.

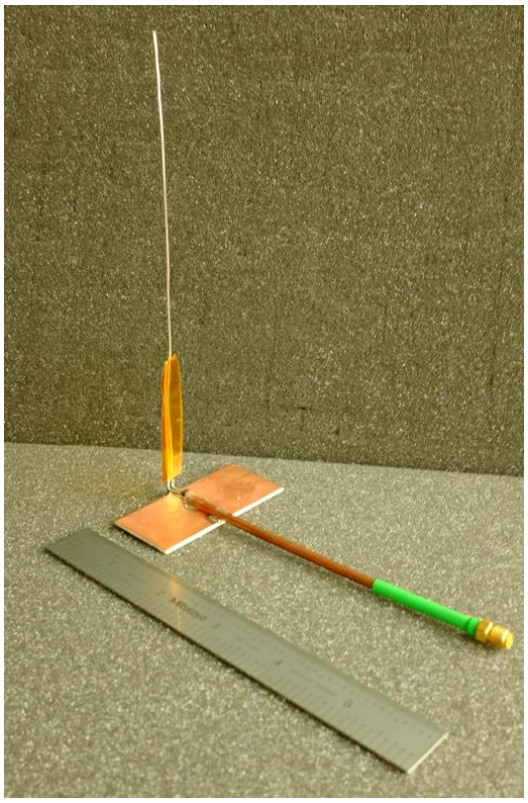

Figure 3.4: 1265 MHz J-Pole Antenna Fed by 0.141 Coax to a 1:1 Balun

Figure 3.5 shows a close up of the 1:1 Balun. The bottom end is 50 ohm 0.141 rigid coax feed by the Balun. The output of the Balun is fed to each arm of the transmission line transformer show at the top of the Balun. Semi-rigid 50 ohm coax cable is used for mechanical rigidity of the antenna test fixture.

Figure 3.6 shows a close up of the shorted end of the J-pole transmission line transformer. Modeling software models the shorted end as a square wire structure with 90 deg bends. During the construction of the antenna,

the bend should not be made square due to the insertion of mechanical stress to the wire. Thus we can see the modeling software can provide confidence the antenna will operate as design, however during construction hand tuning of the antenna may be necessary to compensate for small changes in the Model vs Actual antenna geometry.

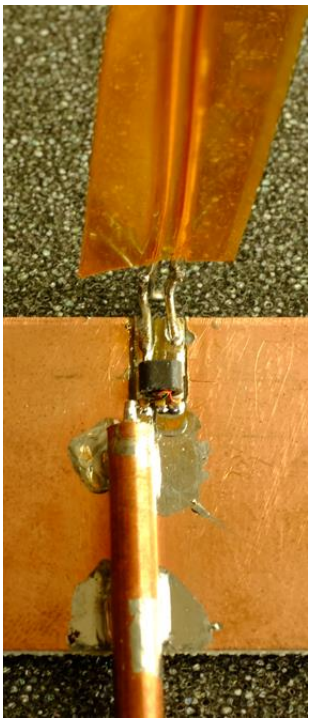

Figure 3.5: Close up of the 1:1 Balun

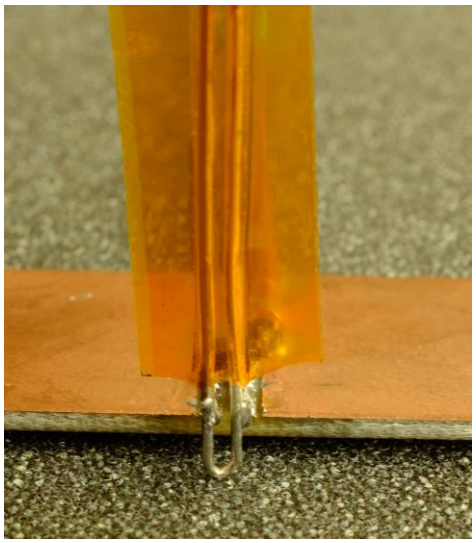

Figure 3.6: Close up of Shorted End of the J-Pole

Test results are shown in Figure 3.7. One must note the Kapton tape provided an increase in the return loss bandwidth from the 2.032 mm spacing of 20 Mhz to double 40 Mhz spacing. The choice of a geometry to support the parallel transmission line can vary from Kapton tape to air dielectric. What is important is the trend for wide impedance bandwidth by the control of the short circuit stub spacing.

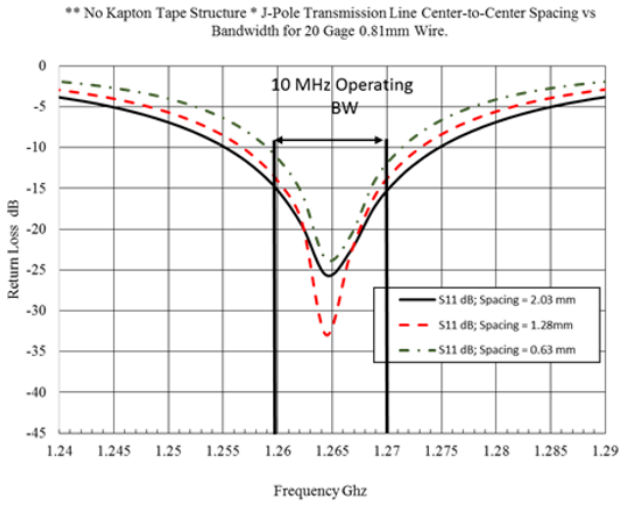

Figure 3.7: Predicted vs Measured Return Loss J-Pole Antenna

Not mentioned is the expected antenna gain of the J-pole. The gain of the J-pole is comparable to a half wavelength dipole of 2.2 dBi. However, the 0.6 dB typical loss of the Balun and unmeasured loss of the Kapton tape at L-band will decrease the antenna gain. However, the gain of an uplink antenna is not very important due to an ability of increased transmission power by a ground station. Also, RF interference from navigation satellites operating over the L-band suggests that the receiver antenna gain should be on the low side.

A L-Band J-pole antenna was modeled and successfully hand built and tested. The 4 times bandwidth provided by the Kapton supported J-pole supports a practical use of this antenna for a Cubesat uplink antenna. Helpful design suggestions such as early bandwidth swings requirement over temperature is required for the antenna to receive as designed over temperature. Temperature stable and low RF loss support structure of the J-pole is recommended to maintain dipole gain. For the final electrical behavior of the antenna, measured peak gain and input return loss measurements over the antenna frequency band in a mock-up Cubesat body structure should be made to assure successful antenna performance in the space environment.

4. S-BAND DOWNLINK PATCH ANTENNA

The patch antenna (Figure 4.1) consists of a radiating patch assembled on a planar structure with the top side containing the radiating patch, a dielectric substrate sandwich separation and a conducting ground plane. The patch can be of any shape, but rectangular, circular and triangle shapes are generally used due to its simple mathematical description. The dielectric constant of the patch should be low (Er ~2.5) so that the patch fringe fields are enhanced which support the radiation characteristic of the patch [6]. The patch radiates at the patch edges because the patch edge voltage vectors are 180º different from one another at the opposite ends of the $\lambda/2$ Y-axis. The 180º electric field difference is what excites the propagation electric field.

Of interest is the patch center showing a voltage flux null of 0 v/m. This condition allows for a DC shorting wire to be placed at this location to discharge any static buildup on the antenna to the spacecraft ground [7][8].

The advantages of the patch are: (i) Lightweight, low volume and low profile, (ii) Low fabrication cost, (iii) Linear or circular polarization are possible with small feed location change, (iv) Radiation in the half plane and extremely low back lobe due to ground plane blockage, and v) Low deployment failure risk. However, typical disadvantages of the patch include: (i) Narrow frequency bandwidth of approximately 2%, (ii) Peak gain < 6-7 dBi, (iii) Poor isolation between the feed and the radiating element (feed changes the antenna pattern), and (iv) Patch surface waves distortion to the patch main beam due to the patch ground plane dimension.

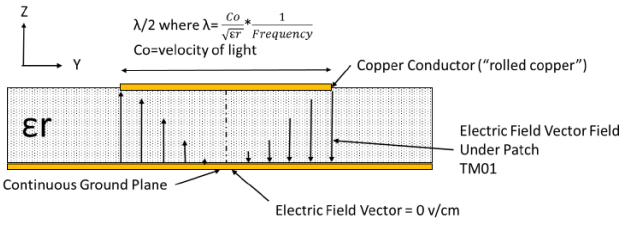

Figure 4.1: Patch Antenna Electric Field [6]

Patch impedance is the ratio of the electric field and current field of the patch. Shown graphically without formula, the impedance can vary exponentially from 0Ω at the patch center to an approximately 180–200Ω at the patch edge. The desired feed point of 50Ω will be off the patch center and can be determined by modeling. There are two practical methods for patch feeds (Figure 4.2): the Microstrip Edge fed and the Pin fed method. The microstrip feed is desirable because the patch and feed are etched on the same plane. However, the microstrip transmission lines will radiate and thus contribute to the total patch far-field pattern. This contribution may not be harmful because the contribution may be small. The pin feed is more desirable since the pin is on the patch side of the board and the patch radiation pattern and RF connection may be advantages to the overall system architecture. However the pin will contribute series inductance to the impedance, thus at higher frequencies this inductance must be compensated.

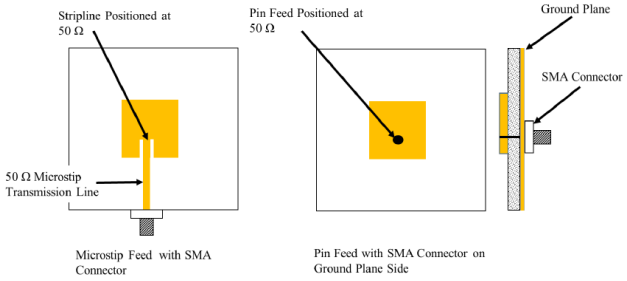

Figure 4.2: Microstrip Feed and Pin Feed for Patch Antennas [9]

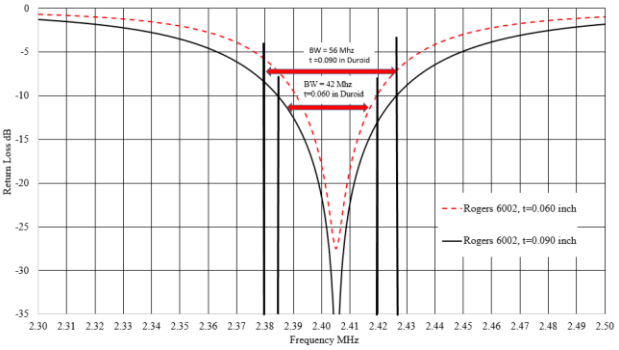

Figure 4.3: Rogers 6002 Thickness vs. Frequency Bandwidth

In the space environment, the antenna is exposed to wide temperature extremes -60C to + 80C, ultra violet and ionized oxygen that will oxidize exposed metal. For frequency stability, the patch dielectric should be of high thermal stability. Orbital Sciences has multiple flight experience with the Rogers Corporation 6002 and 5880 dielectrics. The linear temperature stability of the patch dielectric is desirable to maintain the tuned center frequency of the patch over the temperature extremes found in space. The choice of dielectric thickness is driven by the bandwidth of the patch and dielectric thermal stability. Thicker dielectric produces wider operational bandwidth. For lower thermal stability, wider bandwidth is desirable. There is a danger however, if the substrate is too thick, an unwanted standing wave can be launched within the dielectric.

The tradeoff on thick dielectrics is weight and volume. Figure 4.3 shows an influence of dielectric thickness on radiation bandwidth for Rogers 6002 laminate. A 50% increase in bandwidth was achieved for 0.09 inch compared to 0.06 inch think laminate. For a flight model, the 0.09in thick Rogers 6002 or equivalent is recommended.

4.2 A 5x5 cm Right Hand Circular Polarized S-Band Patch Antenna

Out of several designed, simulated and tested patch antennas, a practical small size patch antenna is presented in this section. The initial design guidance for the antenna included: (i) Operating in the frequency band of 2400 to 2450 MHz, (ii) The far-field polarization shall be RHCP, (iii) The antenna will be optimized to produce a peak gain of > 5.0 dBi, (iv) The use of commercially available "standard" thickness dielectric laminates, and (v) The antenna shall be light weight and fit within a 5 x 5 cm area. The small size was the main objectives of this exercise due to the limited space on a CubeSat surface. Since patch antennas are narrow band devices in the order of 1 to 2 % bandwidth, they usually require 2 to 4 build iterations and antenna range test measurements to get the design to operate at the designed center frequency. Right below, we present an antenna of the first iteration, while someone interested in building one can make small changes for the second final iteration.

For this patch design effort, a patch with the highest gain is desirable. Thus, the Annular Ring (circular ring) antenna or Circular Disk antenna would be a preferred patch choice since it has a slightly higher gain. The typical boresight gain of a patch is between 5 to 6 dBi. For the Annular Ring, the gain can be greater than 7.0 dBi. However, for the ease of tuning, the square patch or rectangular patch is preferred. Additional investigation is required and practical models must be built and tested due to other factors influencing small size patches.

At first, we wanted to see if we could shrink the patch by using higher dielectric material. The variables for this study was: a) Increase in substrate dielectric constant, and b) Increase in patch thickness. A trade study was conducted using PCCAD 6.0 patch software tool to compare the patch peak gain vs dielectric constant vs patch configuration. A comparison (see Table 4.1) was conducted using Rogers TMM6 vs Rogers 6002 dielectric laminates. For this trade, the Rogers 6002 dielectric for a square path produced a higher boresight gain than the TMM6 material. The drop in peak gain is due to the higher dielectric constant of the TMM6 vs the Rogers 6002. The higher dielectric TMM6 will produce a smaller patch, however at the expense of patch gain. In the patch literature, low dielectric material in the range of Er 2.0 to 2.8 is preferred for high gain patches. The higher gain for the low dielectric material is from the concentration of electric field at the patch to dielectric boundary when compared to a spread-out electric field caused by the higher dielectric material.

Table 4.1: Square vs Circular Patch and Dielectric Constant vs Gain

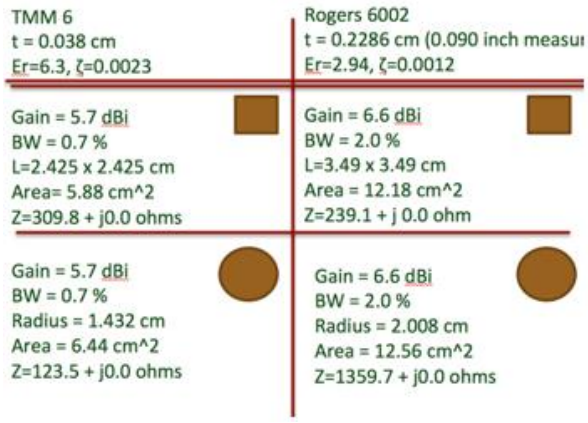

Table 4.2 shows a comparison of the patch surface area vs dielectric constant vs dielectric thickness. The lower height graph (brown color) is more desirable. The comparison shows the thick patch vs high dielectric produces the smallest patch footprint. However, there is a cost in peak gain. This loss in gain for higher dielectric constant was described previously in Table 4.1

Table 4.2: Patch Area vs Dielectric Constant vs Patch Thickness

		TMM 4	TMM6	TMM 10
	Er	4.7	6.3	9.8
Substrate Thickness	0.125in	2.786 cm^2	2.405cm ^2	1.931 cm ^2
	0.275 in	2.485cm^2	2.130cm^2	1.660cm^2
	0.5 in	2.015cm^2	1.668cm^2	1.213cm^2

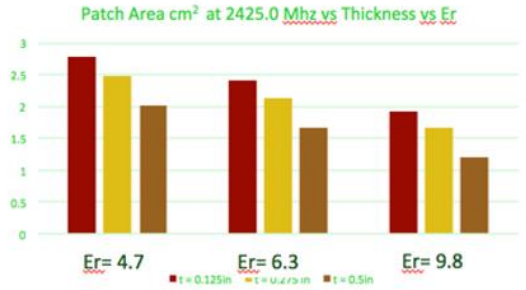

Making small dielectric patch by choosing significantly higher dielectric material is not advised due to peak

gain and bandwidth degradation. Thus, the baseline design for our patch is Rogers 6002 with a dielectric constant of Er = 2.94.

For the RHCP, the patch type is the square patch with chevron corners (Figure 4.4). The chevron cut depth will drive the linear patch to circular polarization. For circular polarization, the chevron cuts are referenced to the feed location. The depth of the chevron cut determines the purity of the polarization. The ratio of RHCP gain vs LHCP gain should be 15 dB or higher for peak axial ratio of less than 3 dB.

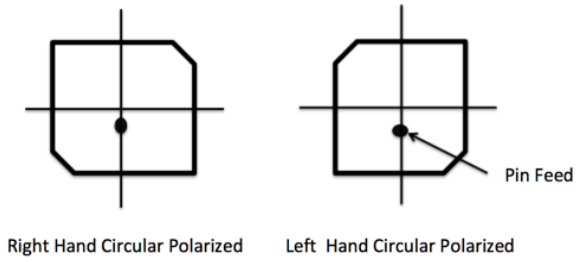

Figure 4.4: Circular Polarization Chevron-Type

The final patch dimensions are shown in Figure 4.5 while chevron length selection, equal to 2.13 cm, is shown in Figure 4.6. The optimum chevron length occurs when the RHCP vs LHCP gain separation is the greatest.

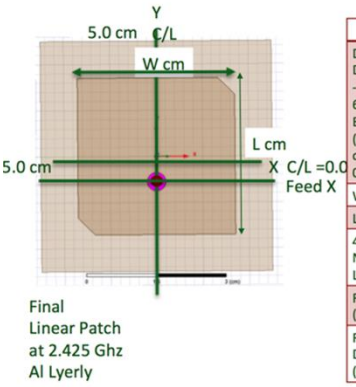

	Units cm	
Dielectric Dimension - Rogers 6002, Er=2.94 cm (1 oz copper) 0.00138 in	5 x 5 x 0.2286	2.5 x 2.5
W cm	3.407	
L cm	3.407	
45 deg Notch Length	0.518	
Feed(X,UY) (	(0.0,- 0.57)	n/a
Feed Drill Diameter (tight fit)	0.127 min	n/a

Figure 4.5: Final Model RHCP 2425 MHz Patch Antenna

The patch return loss performance is shown in Figure 4.7. The best performance for this 5x5 cm patch is -10.0 dB over the bandwidth outlined in red boundaries. This match for this patch is determined by feed position only and can be adjusted in the next design iteration to bring the minimum closer to 2425 MHz. The Final Model RHCP patch antenna pattern is shown in Figure 4.8. The antenna pattern shows the boresight gain to be about 6.0 dBi at 2425.0 MHz. The plot includes a family of Phi cuts from 0 to 180.0°. The Phi cuts show the axial ratio pattern will vary due to the asymmetry of the patch ground plane.

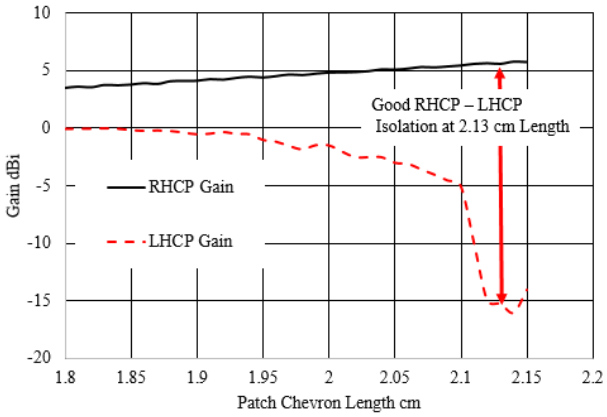

Figure 4.6: Chevron Length vs RHCP and LHCP Gain

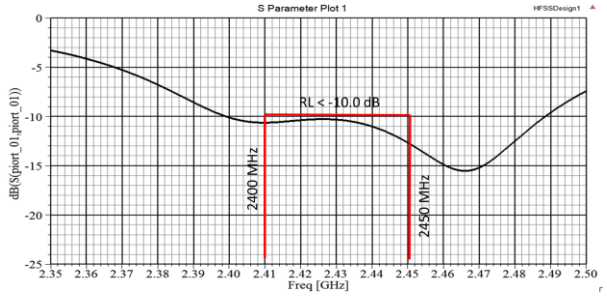

Figure 4.7: Return Loss vs Frequency

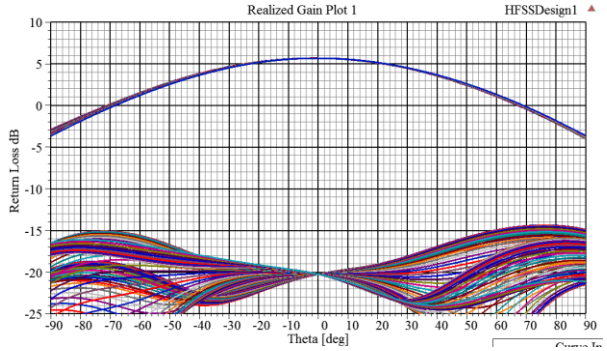

Figure 4.8: Model RHCP Gain vs Theta vs Phi

The patch was machined according to above provided specification with a SMA connector soldered to the back side of the patch. The antenna characteristics was measured at the Northrop Grumman anechoic chamber. Figure 4.9 shows the antenna mounted on a panel with flat Emerson and Cummings Absorber panel. This

panel attenuates any RF plane wave by approximately 30 dB.

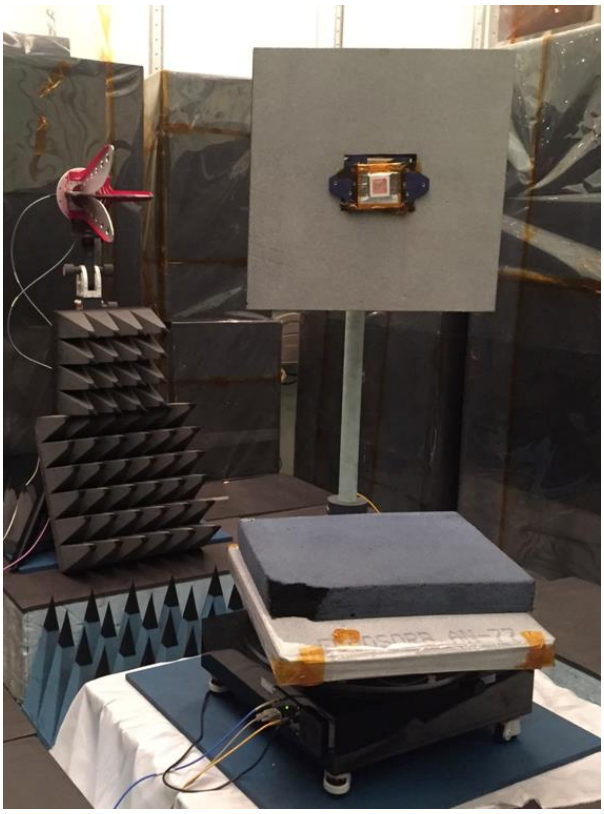

Figure 4.9: RHCP Patch in Antenna Testing Setup

Figure 4.10 shows the tested patch RHCP pattern cut in green overlaid over the model pattern cut in light purple. The measured pattern has good agreement to the model pattern out to +/- 40 deg in Theta. The LHCP cross polarization is approximately 8 dB down from the RHCP copol. The measured antenna return loss, shown in Figure 4.11, shows the patch is tuned to 2500.0 Mhz. This is 25.0 MHz too high.

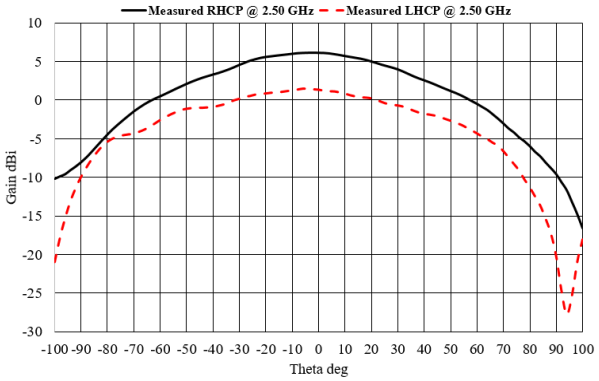

Figure 4.10: Measured RHCP Patch Antenna at 2500 MHz

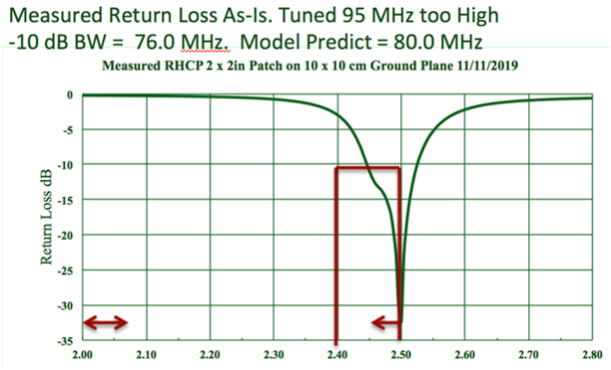

Figure 4.11: Measured Return Loss (Resonance is at 2500 MHz)

As expected, in the first design iteration, the as-build patch is not tuned correctly. The patch was designed to operate at 2425.0 Mhz with good LHCP rejection at that frequency. The good return loss occurs at 2500.0 Mhz, this indicates that the patch is too small. It can be tuned easily by making is slightly larger. The LHCP or cross polarization suppression is only 8 dB. This indicates that further models must be built to reach higher cross polarization suppression. However, for such a small S-band patch antenna one can easily achieve gain above 5dBi. Hence, expect to have 3 to 4 design iterations for the patch antenna. For this exercise the antenna is operating fairly close to its operating frequency.

4.3 Experimental S-Band Fractal Patch Antenna

This section evaluates another possibility of shrinking antenna size through fractalization of patch shape. The area saved by the reduced patch area can make room for an additional sensor or component. This method has shown the ability to reduce patch area with a small reduction in antenna bandwidth. This section explores Minkowski fractalization of a linear patch.

In this exercise, we wanted to compare two designs to show the effect of fractalization. Both, square and fractal patch were designed for FR4 material with oversized ground plane in order to eliminate the ground influence. Patch designs are shown on Figure 4.12 with 1st iteration Minkowski patch.

Gain prediction for the fractal patch is shown in Figure 4.13. This is a single plane cut of a single Phi=0.0 degrees. This gain is about 0.5dB lower than the gain of the “control”, square patch gain. This might sound not much but for a small CubeSat this may not be acceptable. One can also expect that this gain can be even lower for a built patch prototype with smaller

ground plane. Figure 4.14 shows a comparison of the square patch vs fractal patch return loss. The impedance bandwidth graph shows the decrease in impedance bandwidth for the fractal patch.

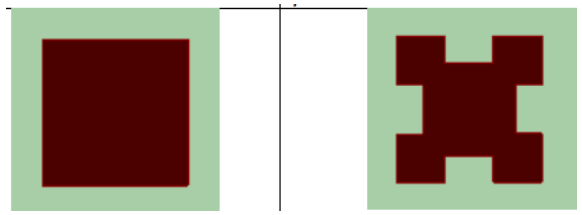

Figure 4.12: Model Patch Transformed to the 1st Minkowski Patch

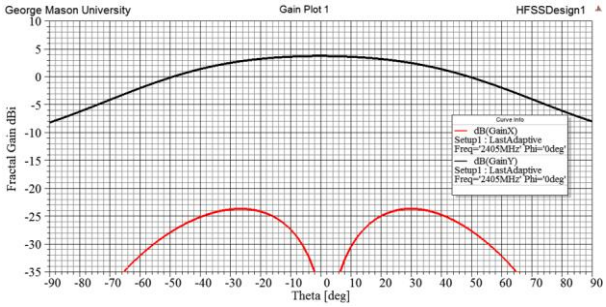

Figure 4.13: Model Fractal Antenna Gain and Cross Polarization at 2504 MHz

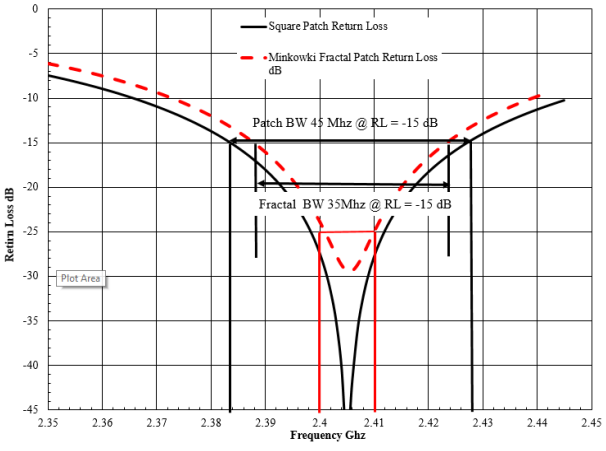

Figure 4.14: Bandwidth Contraction - Model Square Patch vs Minkowski Patch Antenna

In the next step, we built both patches according to dimensions provided in Table 4.3. Both antennas were simulated with ANSYS HFSS and tested in an anechoic chamber with ANSYS HFSS simulated results shown in Table 4.3

Table 4.3: Square Patch vs Minkowski Patch Dimensions and Simulation Performance Summary

Parameter	Square Patch	Minkowski Patch
Dimensions (mm) FR4 substrate: 152.4x152.4x 3.175 Er=4.4, Tau=0.02	Patch size: 27.3 x 26.3 Feed point=5.0 from center Tuned to 2405 MHz	Patch size: 24.5 x 24.5 Feed point=4.25 from center
Peak Gain at 2405 MHz FR4 tau = 0.02 (ANSYS HFSS)	4.8 dBi	3.9 dBi
Peak Gain at 2405 MHz FR tau = 0.009 (ANSYS HFSS)	5.4 dBi	4.92 dBi
-15 dB Return Loss Bandwidth (ANSYS HFSS)	44.0 MHz	35.0 MHz

Typical test result from RF range is shown in Figure 4.15 and Figure 4.16. Comparing the measured square patch to the fractal patch, the patterns are almost identical except for ~1 dB drop in the peak gain which was predicted in HFSS. However, the fractal patch has higher bandwidth than the square patch. This can improve when a better impedance matching is implemented.

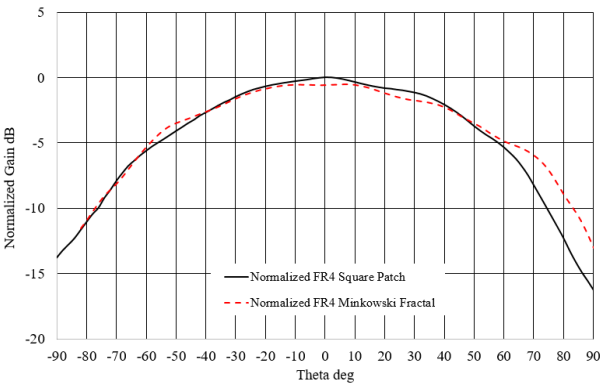

Figure 4.15: Measured Normalized Gain of Square Patch (Solid Line) and Minkowski Patch (Dashed Line)

In summary, we have shown what kind of design considerations and problems a designer has to go through to design, build and test S-band patch antenna. This process is elaborate with at least 3-5 iterations

needed to achieve design objectives. Designing a small 5x5 cm patch is achievable, however designing a fractal patch is significantly more complex and will almost certainly provide significantly worse results in terms of gain. Such a drop in gain may not justify savings of an additional small area when compared to a square patch. For a CubeSat mission, recorded in our testing the 0.9 dB drop in gain may not be acceptable to the communication engineer. Further investigation is needed if one decides to design a fractal patch and should expect that this process will be expensive in time and material when space graded substrate such as Rogers 6002 is used and multiple iterations are required. An access to an anechoic chamber will also impact the expenses and time.

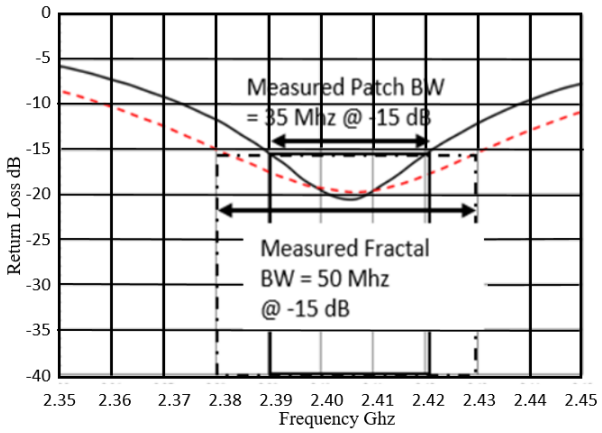

Figure 4.16: Measured Return Loss for Square Patch (Solid Line) and Minkowski Patch (Dashed Line)

5. SUMMARY

The study presented in this paper should be considered as a starting point, or an initial guidance, in the development of final antennas for academic CubeSats. As mentioned, about 3-4 design-build-test iterations are needed to finalize a design. Through this initial study, we showed an influence of other factors a communications engineer must take into consideration. We also provided remedies/tips which will improve antenna performance within given frequency band and mitigate these factors.

Acknowledgements

The authors would like to thank the Northrop Grumman Corporation for allowing an access to their anechoic chamber and instrumentation. This paper would not be possible without their generosity.

References

1. Balanis, C., Modern Antenna Handbook. John Wiley and Sons, 2008.

2. The ARRL Antenna Book. American Radio Relay League, 2019.

3. Rahman-Samii, Y., Vignesh, Kovitz, J. M., “For Satelites, Think Small, Dream Big: A review of recent antenna developments for CubeSats.” IEEE Antennas and Propagation, 59(2), 22-30, 2017.

4. Busch, S., “Robust, Flexible and Efficient Design for Miniature Satellite Systems,” Ph.D Thesis, University of Wuerzburg, 2016.

5. Beggerow, H., "Zeppelin Antenna" (PDF). Patent 1909. Retrieved 28 January 2016.

6. Bhartia, P., Bahl, I., Microstrip Antennas. Artech House, 1980.

7. DeSantos, G., EMI/EMC Grounding Requirements for Spacecraft. Dulles, Virginia: Orbital Sciences, 2019.

8. DOD-STD-1685. (n.d.). Electrostatic Discharge Control Handbook for Protection of Electrical and Electronic Parts and Assemblies. DOD.

9. Balanis, C., Antenna Theory, 3rd Edition, John Wiley, 2005.